

# Reduction of $B_1$ Inhomogeneity Using $B_1$ Rectifying Fin at High Fields

Y. Kaneko<sup>1</sup>, H. Habara<sup>1</sup>, Y. Soutome<sup>1</sup>, and Y. Bito<sup>1</sup>

<sup>1</sup>Central Research Laboratory, Hitachi, Ltd., Kokubunji-shi, Tokyo, Japan

## Introduction

$B_1$  inhomogeneity in a human body increases as the strength of static magnetic field increases and the RF wavelength becomes smaller. Recently, various RF control methods have been developed to reduce  $B_1$  inhomogeneity. For example, some methods involve devices such as dielectric pads [1,2] or coupling coils [3,4], or techniques such as  $B_1$  shimming [5,6]. However,  $B_1$  inhomogeneity still remains in some cases of abdominal imaging, and a more effective method for reducing  $B_1$  inhomogeneity is required. In this paper, we have proposed a new method to reduce  $B_1$  inhomogeneity using a “ $B_1$  rectifying fin” combined with  $B_1$  shimming. This method can reduce  $B_1$  inhomogeneity less than 2-port  $B_1$  shimming used in some commercial MRI, and moreover, the fin has a simple structure with no capacitor or inductor. The effect of the fin on  $B_1$  inhomogeneity was analyzed using both finite-difference time-domain (FDTD) simulation and experiments.

## Method

**Design:** The fin consists of a thin sheet with conductive property. In an electromagnetic field, the fin can change the magnetic flux around it, that is, it can create high or low density of the flux. This is because an electrical current flows in a direction which counters the magnetic flux across the fin. The spatial distribution of the  $B_1$  field can be controlled by using this phenomenon in an appropriate manner. Figure 1 illustrates an example of the  $B_1$  rectifying fin arranged to reduce  $B_1$  inhomogeneity. The fins around the body are arranged like a windmill, taking into consideration the phenomena of RF propagation from the RF transmit coil to the abdomen, and the position of larger and smaller  $B_1$  regions in the abdomen. Specifically, the fins are positioned near the abdomen where the  $B_1$  value is larger, and the edges of the fins are positioned near the region of the smaller  $B_1$ . There is no need, in principle, to use a capacitor or inductor with this method.

**Simulation:** The effect of the  $B_1$  rectifying fin was confirmed through numerical analysis of the electromagnetic field. The spatial distribution of the  $B_1$  field in the phantom was calculated using an electromagnetic simulation tool (xFDTD<sup>®</sup>). A 2-port birdcage coil was used for RF transmission, and the RF frequency was 128 MHz. The phantom size (xy plane) was 350 x 200 mm. The conductivity and relative permittivity of the phantom were 0.55 S/m and 50, respectively. Four fins were set around the phantom. In this case, the fins covered 50 % of the surface of the phantom, and the gap between the fin and the surface was 20 mm. A  $B_1$  homogeneity value ( $U_{SD}$ ) was used to evaluate  $B_1$  inhomogeneity, and  $U_{SD}$  = standard deviation of  $B_1$  / average of  $B_1$ .

**Experiment:** A human abdominal imaging experiment was conducted, using a 3T MR scanner (Varian INOVA). The  $B_1$  rectifying fins were set around the abdomen, and the placement of the fins (coverage percentage and gap) was the same as that in the simulation case. Copper mesh sheets (0.1 mm thick) were used as the material for the  $B_1$  rectifying fins for this experiment, and their weight was very small (~ 0.1 kg). The mesh sheets were put on a synthetic rubber sheet (20 mm thick), and the rubber sheet was set around the lower abdomen, like a torso coil.  $B_1$  mapping was accomplished using the double-angle method in order to evaluate the effect of the fins. The sequence parameters were FOV = 450 mm, TR/TE = 5000/6.7 ms, matrix = 128 x 64, thickness = 10 mm, flip angle = 60, 120 degrees.

## Results and Discussion

Figure 2 shows the simulation results of the spatial distribution of the  $B_1$  field in the phantom. The  $B_1$  map in case (b), with  $B_1$  shimming alone, is more homogeneous than that in case (a), with a quadrature drive (QD). The  $B_1$  map is the most homogeneous in case (c), in which both the  $B_1$  rectifying fin and  $B_1$  shimming were used. Figure 2 (d) represents the  $B_1$  homogeneity value ( $U_{SD}$ ) and the average of  $B_1$ . The  $B_1$  average values were normalized with the value in case (a). The values of  $U_{SD}$  for (a)(b)(c) are 0.224, 0.164, and 0.126, respectively, and  $U_{SD}$  decreases when both the  $B_1$  rectifying fin and  $B_1$  shimming are used. The average values of  $B_1$  for (a)(b)(c) are 1, 0.97, and 0.95, respectively, and the average of  $B_1$  remains static. The  $B_1$  rectifying fin doesn't reduce the average of  $B_1$ , which means that the fin has the effects of both enhancing and diminishing the magnetic flux. It was confirmed that the  $B_1$  rectifying fin can reduce  $B_1$  inhomogeneity, while maintaining the average value of  $B_1$ . Figure 3 shows the experimental results of the spatial distribution of  $B_1$  in a human abdomen. The values of  $U_{SD}$  for (a)(b)(c) are 0.222, 0.168, and 0.112, and the average of  $B_1$  for (a)(b)(c) are 1, 1.00, and 0.99, respectively. The  $B_1$  rectifying fin can contribute to reducing  $B_1$  inhomogeneity as shown in the simulation results. It is suggested that the  $B_1$  rectifying fin can be useful for reducing  $B_1$  inhomogeneity at higher magnetic field, more than 3 T.

## Conclusion

We have proposed a new method using a  $B_1$  rectifying fin combined with  $B_1$  shimming. Both FDTD simulation and experiments were conducted, and we confirmed that the  $B_1$  rectifying fin, used with  $B_1$  shimming, was more effective in reducing  $B_1$  inhomogeneity than  $B_1$  shimming alone.

## Reference

- [1] Schmitt M et al. ISMRM 2004; 11: 197. [2] Kendra MF et al. J Magn Reson Imaging 2008; 27: 1443-1447. [3] Schmitt M et al. ISMRM 2005; 13: 331. [4] Wang S et al. ISMRM 2007; 15: 3275. [5] Nistler J et al. ISMRM 2007; 15: 1063. [6] Hajnal JV et al. ISMRM 2008; 16: 496.

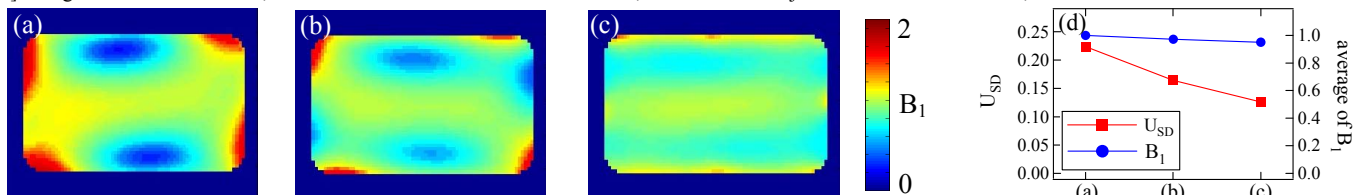


Figure 2 Simulation results with phantom.  $B_1$  map for (a) QD, (b)  $B_1$  shimming, (c)  $B_1$  rectifying fin +  $B_1$  shimming. (d)  $U_{SD}$  and average of  $B_1$ .

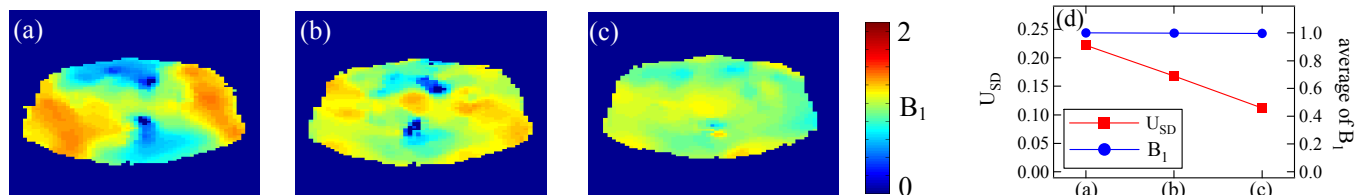


Figure 3 Experimental results with human abdomen.  $B_1$  map for (a) QD, (b)  $B_1$  shimming, (c)  $B_1$  rectifying fin +  $B_1$  shimming. (d)  $U_{SD}$  and average of  $B_1$ .

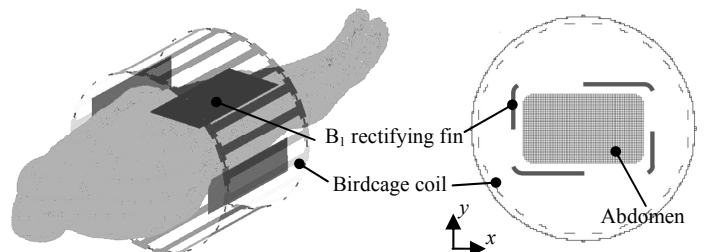


Figure 1 Schematic of  $B_1$  rectifying fin.